New compounds with MgAgAs-type structure: NbIrSn and NbIrSb

1998 J. Phys.: Condens. Matter 10 7843

(http://iopscience.iop.org/0953-8984/10/35/016)

J. Phys.: Condens. Matter **10** (1998) 7843–7850. Printed in the UK PII: S0953-8984(98)94259-X

New compounds with MgAgAs-type structure: NbIrSn and NbIrSb

Heinrich Hohl, Art P Ramirez, Claudia Goldmann†, Gabriele Ernst, Bernd Wölfing and Ernst Bucher†

Lucent Technologies, Bell Laboratories, 700 Mountain Avenue, Murray Hill, NJ 07974-0636, USA

Received 15 May 1998

Abstract. NbIrSn and NbIrSb crystallize in a cubic MgAgAs-type structure with lattice parameters of 617.76(2) and 614.97(2) pm, respectively. Both compounds exhibit incongruent melting behaviour. NbIrSn is a p-type semiconductor with an energy gap of 0.28 eV. At room temperature, it has a Seebeck coefficient of $+176\ \mu V\ K^{-1}$ and a resistivity of 1.1 Ω cm. NbIrSb is metallic with $S = +3.5\ \mu V\ K^{-1}$ and $\rho = 1.5 \times 10^{-3}$ Ω cm at room temperature. The formation of the solid solutions $NbIrSn_{1-x}Sb_x$ has been confirmed.

1. Introduction

A number of ternary compounds with equiatomic composition ABX may be formed by combining a transition metal A from the left-hand side of the periodic table (titanium or vanadium group elements), a transition metal B from the right-hand side of the periodic table (iron, cobalt, or nickel group elements), and one of the main group elements X = Ga, Sn, or Sb. These compounds crystallize either in a hexagonal Fe_2P-type structure (space group $P\bar{6}2m$, No 189) or in a cubic MgAgAs-type structure (space group $F\bar{4}3m$, No 216; also called LiAlSi-type or MgCuSb-type structure).

Among these compounds, 10 gallides, 18 stannides, and 11 antimonides are listed in *Pearson's Handbook* [1]. The data in the handbook are based on studies by Dwight *et al* [2], Jeitschko [3], and some other groups [4–6]. Further stannides and antimonides have been reported since then [7–9]. In this paper, we will present two more members of this family of compounds, NbIrSn and NbIrSb, both of which crystallize in a cubic MgAgAs-type structure.

Figure 1 shows the unit cell of this structure, assuming that the composition of the compound is given by ABX. One unit cell holds four formula units, with A atoms in the 4b $(1/2, 1/2, 1/2)$ positions, B atoms in the 4c $(1/4, 1/4, 1/4)$ positions, and X atoms in the 4a $(0, 0, 0)$ positions. The structure may be regarded as four interpenetrating fcc lattices: a lattice of A atoms and a lattice of X atoms, together forming a rock-salt structure, and a lattice of B atoms occupying the centre of every other cube. The centres of the remaining cubes remain empty, thereby forming a fcc lattice of vacancies. When filling up these vacancies with additional B atoms we obtain a 'Heusler compound' AB_2X with a cubic

† Also at: Universität Konstanz, Fakultät für Physik, Fach X 910, D-78457 Konstanz, Germany.

0953-8984/98/357843+08$19.50

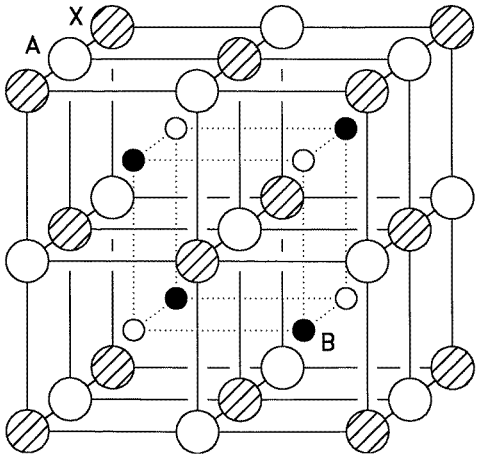

Figure 1. The unit cell of an ABX compound with a cubic MgAgAs-type structure. The small circles represent vacancies.

Table 1. Lattice parameters of gallides ABGa with a cubic MgAgAs-type structure, in picometres [1–4]. No compounds are known with A = V, Nb, Ta. The label 'hex' marks compounds with a hexagonal Fe_2P-type structure.

	Fe	Ru	Os	Co	Rh	Ir	Ni	Pd	Pt
Ti	—	—	—	—	611	—	hex	—	—
Zr	—	—	—	hex	hex	—	hex	—	hex
Hf	—	—	—	hex	hex	—	hex	—	hex

Table 2. Lattice parameters of stannides ABSn with a cubic MgAgAs-type structure, in picometres [1–8]. The label 'hex' marks compounds with a hexagonal Fe_2P-type structure.

	Fe	Ru	Os	Co	Rh	Ir	Ni	Pd	Pt
Ti	633	—	—	600	620	619	593	—	616
Zr	—	—	—	hex	hex	hex	611	632	634
Hf	—	—	—	hex	hex	hex	608	630	631
V	—	—	—	—	—	—	—	—	—
Nb	—	—	—	595	613	618*	—	—	—
Ta	—	—	—	—	—	617	—	—	—

*This work.

$MnCu_2Al$-type structure†. Compounds with a cubic MgAgAs-type structure are therefore often called 'semi-Heusler' or 'half-filled Heusler' compounds.

An updated compilation of the ternary intermetallic compounds ABX formed by the above-mentioned elements is given in tables 1–3. The tables list a total of 10 gallides, 22 stannides, and 22 antimonides, and the lattice parameters of the compounds with a cubic

† The existence of a Heusler compound AB_2X does not in general imply the existence of the corresponding half-filled Heusler compound ABX and vice versa. Also, the existence of both compounds does not necessarily imply the existence of a continuous solid-solution series $AB_{2-x}X$ ($0 \leqslant x \leqslant 1$) [3].

Table 3. Lattice parameters of antimonides ABSb with a cubic MgAgAs-type structure, in picometres [1–9].

	Fe	Ru	Os	Co	Rh	Ir	Ni	Pd	Pt
Ti	596	616	—	588	609	—	587	—	—
Zr	—	633	—	607	626	—	—	—	—
Hf	—	631	—	604	624	—	—	—	—
V	583	607	—	580	—	—	579	—	—
Nb	595	614	—	590	612	615*	—	—	—
Ta	—	614	—	588	—	—	—	—	—

*This work.

MgAgAs-type structure are given†. To achieve consistency among various sources, these data have been rounded to full picometres.

The total number of nominal valence electrons per formula unit, z, appears to be a useful criterion as regards the occurrence of specific crystal structures in these materials [4, 10]. Compounds with a hexagonal Fe_2P-type structure are found for $z = 16$–17, with a preference for $z = 17$. The cubic MgAgAs-type structure covers the range $z = 16$–20, and there is a pronounced peak at $z = 18$. (Ternary aluminides of the A and B transition metals are consistent with these guidelines, and also show that, for $z = 15$–16, another hexagonal structure, the $MgZn_2$-type one, becomes preferred [4].)

TiNiSn, ZrNiSn, and HfNiSn are some of the better known compounds with a cubic MgAgAs-type structure. They are narrow-band-gap semiconductors with an unusual band structure and they show promising thermoelectric properties [11–15]. As can be seen from the electronic configurations of Ti ($3d^24s^2$), Ni ($3d^84s^2$), and Sn ($5s^25p^2$), each of the compounds holds a total number of 18 valence electrons. The same 'magic number' of valence electrons is obtained for an equiatomic combination of Nb ($4d^45s^1$), Ir ($5d^76s^2$), and tin. Therefore, it seems likely that the compound NbIrSn should form easily and that it should crystallize in a cubic MgAgAs-type structure. For equiatomic combinations of niobium and iridium with Ga ($4s^24p^1$) or with Sb ($5s^25p^3$) we find $z = 17$ and 19 valence electrons, respectively. These compounds, if they form at all, are expected to crystallize in a Fe_2P-type and in a MgAgAs-type structure, respectively.

We prepared compounds of nominal composition NbIrX (X = Ga, Sn, Sb) and found that both the stannide and the antimonide are formed. We also prepared alloys of the latter two compounds, $NbIrSn_{0.99}Sb_{0.01}$ and $NbIrSn_{0.5}Sb_{0.5}$. The structural parameters and the thermoelectric properties of the materials will be discussed.

2. Experimental procedure

Compounds of nominal composition NbIrX (X = Ga, Sn, Sb) and $NbIrSn_{1-x}Sb_x$ ($x = 0.01$, 0.5) were made from the following elements: Nb (MRC, grade marz, rod); Ir (Gallard Schlesinger, 4N8, powder); Ga (Eagle Picher, 4N, lump); Sn (Cominco, 5N, pellets); and Sb (Gallard Schlesinger, 5N, lump). A fine niobium powder was obtained by filing the niobium rod with a clean steel file. The filings were passed through a sieve (mesh 100, 0.15 mm) and file abrasions removed with a magnet. The tin pieces were etched in hydrochloric acid prior to use.

† More compounds are, of course, found if further elements are taken into consideration. The actinides thorium and uranium, e.g., may in most cases replace zirconium or hafnium [4].

Stoichiometric amounts of niobium, iridium, and antimony (where required) were ground together in a mortar and pressed into pellets using a pressure of 20 kN cm^{-2}. The pellets and stoichiometric amounts of gallium or tin (where required) were double sealed in evacuated quartz ampoules and heated to 1000 °C for one day. During this first treatment, the gallium or tin pieces which were placed on top of the pellets melted into the pellets and were absorbed by chemical reaction. The products were ground, repelletized, and annealed for another day at 1000 °C, a procedure that was repeated three more times with a slightly higher temperature of 1050 °C in the final step. A diamond blade saw was used to cut the resulting pellets into bars of about $1.5 \times 1.5 \times 10$ mm^3 in size.

Powder diffraction patterns of the samples were recorded on a Philips PW-1710 powder diffractometer. We scanned the 2θ range 20–100° in steps of 0.02°, counting for 15 seconds at each step. LaB_6 was used as the standard. The Seebeck coefficient was measured with an MMR SB-100 Seebeck controller in the range 80–480 K. The SB-100 measures the thermopower with respect to copper, and the data have been corrected for the contribution from the copper electrodes. Linear four-probe set-ups were used for the resistivity measurements at low (4–360 K) and at elevated (290–700 K) temperatures. The resistivity measurements above room temperature were performed in an argon atmosphere. Silver epoxy was used to attach contacts to the samples in all of the transport measurements.

3. Results and discussion

The powder diffraction pattern of the NbIrGa sample shows two phases, both of which have been described in the literature previously [16]. The pattern is dominated by a $Nb_{0.30}Ir_{0.35}Ga_{0.35}$ phase which is hexagonal, but different from the Fe_2P-type one. There is also a considerable amount of a tetragonal $Nb_{0.25}Ir_{0.23}Ga_{0.52}$ phase present. No elements or binary phases of the elements are found in the pattern, and repeated intermediate grinding does not reduce the amount of the tetragonal phase.

The powder diffraction patterns of NbIrSn and of NbIrSb are shown in figure 2. Both compounds crystallize in cubic structure, and lattice parameters of 617.76(2) and 614.97(2) pm, respectively, are found by a least-squares refinement. Intensity calculations confirm a cubic MgAgAs-type structure. Since there are four formula units per unit-cell volume, the x-ray densities of the compounds are 11.38 and 11.62 g cm^{-3}, respectively. The overall density of the samples, which was calculated from the mass and the volume of the pellets and therefore reflects the sample porosity, is about 70–75% of the x-ray density.

NbIrSn is easily obtained in a phase-pure form. Even at reaction temperatures as low as 850 °C, a single-phase diffraction pattern is already found after repelletizing the sample just once. Impurity phases are much more of a concern in the preparation of NbIrSb, and several intermediate steps of grinding and repelletizing are necessary to prepare this compound. Furthermore, it appears advantageous to use very fine metal powders and to have a reaction temperature of about 1000 °C. The powder diffraction pattern of NbIrSb in figure 2 shows the sample with the lowest impurity content.

The alloys $NbIrSn_{0.99}Sb_{0.01}$ and $NbIrSn_{0.5}Sb_{0.5}$ form just as well as NbIrSn and are single phase. A lattice parameter of 616.46(2) pm is found for $NbIrSn_{0.5}Sb_{0.5}$. This value corresponds well with the mean of the lattice parameters of NbIrSn and NbIrSb. According to Vegard's law [17], a linear dependence of the unit-cell volume on composition indicates the formation of a solid solution by random substitution of atoms or ions†. We only prepared a few members of the series $NbIrSn_{1-x}Sb_x$, but there is little doubt that the solid-solution

† In cubic compounds, this implies a linear dependence of the lattice parameter on the composition.

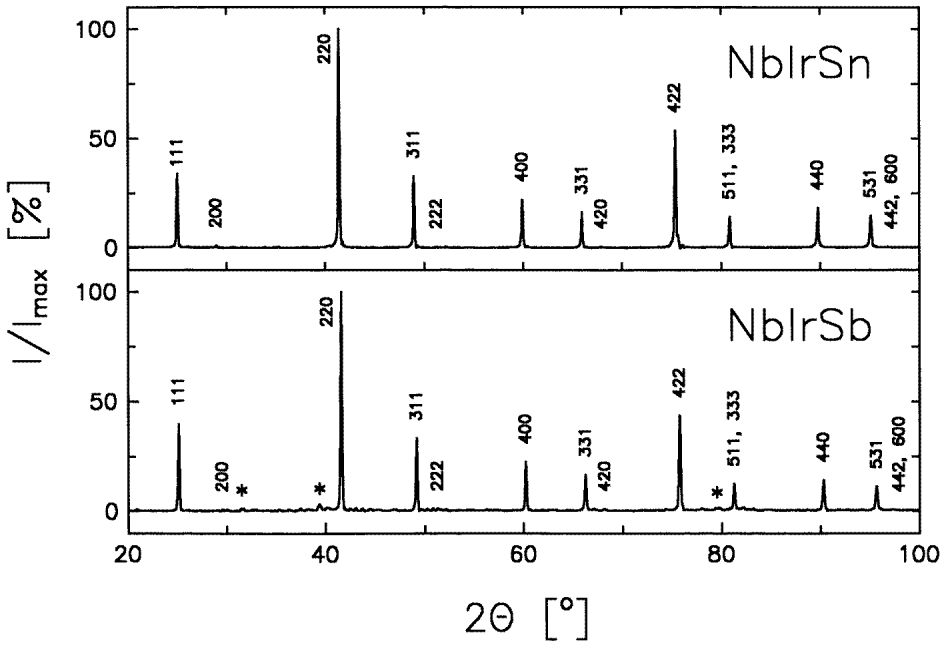

Figure 2. Powder diffraction patterns of NbIrSn and NbIrSb, recorded with Cu Kα radiation. Both compounds crystallize in a cubic MgAgAs-type structure and contain four formula units per unit-cell volume. The lattice parameters are 617.76(2) and 614.97(2) pm, respectively. Impurity peaks are marked by asterisks.

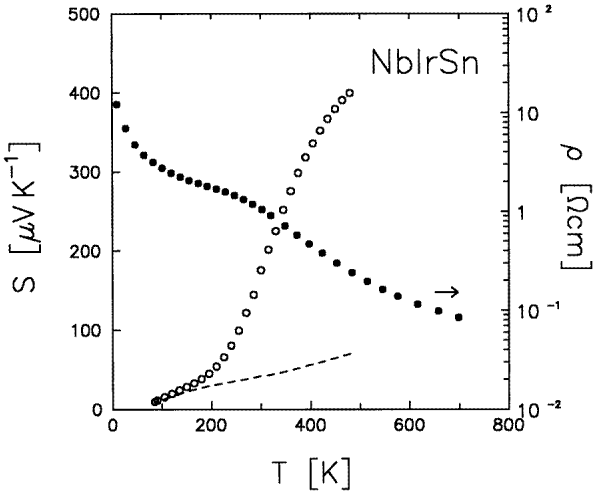

Figure 3. The Seebeck coefficient (○) and resistivity (●) of NbIrSn. The dashed line shows the Seebeck coefficient of $NbIrSn_{0.99}Sb_{0.01}$.

series covers the entire range $0 \leqslant x \leqslant 1$.

Attempts to prepare NbIrSn and NbIrSb by arc melting of the elements have been unsuccessful. We therefore melted pellets of the compounds which had been obtained by

solid-state reactions. The resulting buttons have a multiphase composition. This shows that both compounds exhibit incongruent melting behaviour and cannot be obtained from a melt.

Figure 3 shows the Seebeck coefficient and the resistivity of NbIrSn as a function of temperature. NbIrSn is a p-type conductor with a Seebeck coefficient of $+176\ \mu V\ K^{-1}$ at room temperature. The overall behaviour of the resistivity curve is semiconductor-like and the room temperature resistivity is 1.1 Ω cm. Thermally activated behaviour

$$\rho \propto \exp\left(\frac{E_g}{2k_B T}\right) \tag{1}$$

with an energy gap of $E_g = 0.28$ eV is found above 400 K. The substitution of antimony for 1% of the tin atoms has only little effect on the resistivity ($\rho_{300\,K} = 1.9$ Ω cm). The Seebeck coefficient, however, is significantly reduced as can be seen from the dashed line in figure 3. Because antimony acts as an n-type dopant in this compound, it causes a negative contribution to the Seebeck coefficient which partially cancels the positive Seebeck coefficient of NbIrSn.

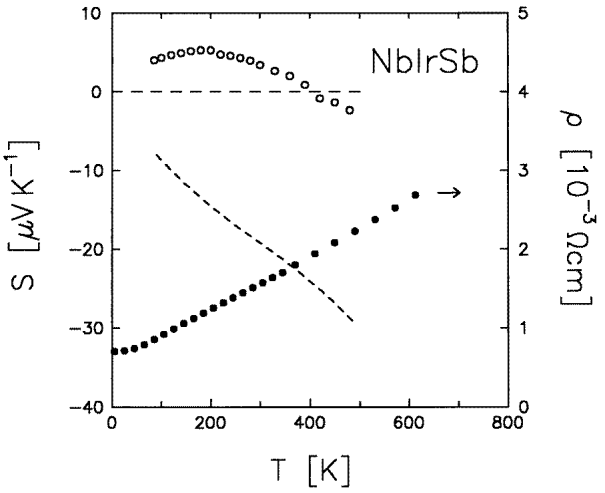

Figure 4. The Seebeck coefficient (○) and resistivity (●) of NbIrSb. The dashed line shows the Seebeck coefficient of $NbIrSn_{0.5}Sb_{0.5}$.

The temperature dependence of the resistivity of NbIrSb (figure 4) resembles that for a metal. But with a room temperature resistivity of 1.5×10^{-3} Ω cm and a residual resistivity ratio of 2.2, this compound might also represent a degenerate semiconductor. The resistivity of $NbIrSn_{0.5}Sb_{0.5}$ ($\rho_{300\,K} = 1.5 \times 10^{-3}$ Ω cm; RRR = 1.2) is very similar to that of NbIrSb.

In the free-electron model [18], the Seebeck coefficient of a metal or a degenerate semiconductor in the phonon scattering region (i.e. well above the residual resistivity region) is given by

$$S = \pm\frac{\pi^2 k_B}{e}\frac{T}{T_F}. \tag{2}$$

This equation may be rewritten as

$$S = \pm 850(T/T_F)\ \mu V\ K^{-1}.$$

The sign of the thermopower corresponds to the sign of the charge carriers, and T_F is the Fermi temperature of the system which depends on the carrier concentration n according to

$$T_F = 4.23 \times 10^{-11} \times (n/\mathrm{cm}^{-3})^{2/3}\ \mathrm{K}.$$

If we assume that each antimony atom contributes one valence electron to the conduction band, we obtain a carrier concentration of $n = 4/a^3 = 1.7 \times 10^{22}$ cm^{-3} for NbIrSn, and $n = 8.5 \times 10^{21}$ cm^{-3} for $NbIrSn_{0.5}Sb_{0.5}$. According to the free-electron approximation (2), the Seebeck coefficient is expected to depend linearly on the temperature with slopes of $dS/dT = -0.030\ \mu V\ K^{-2}$ and $-0.048\ \mu V\ K^{-2}$ for NbIrSn and $NbIrSn_{0.5}Sb_{0.5}$, respectively.

Figure 4 shows the measured Seebeck coefficient of NbIrSb. Above 280 K, the curve has a linear temperature dependence with a slope of $-0.032\ \mu V\ K^{-2}$. This value is in good agreement with the free-electron model. We reach the same conclusion for $NbIrSn_{0.5}Sb_{0.5}$ (the dashed line in figure 4), which has a slope of $-0.051\ \mu V\ K^{-2}$ between 80 and 480 K.

The free-electron model does not, however, explain the upturn to positive values in the Seebeck coefficient of NbIrSb below room temperature. It is rather likely that this additional contribution to the Seebeck coefficient is caused by the phonon-drag effect [18]. Unlike the 'diffusion thermopower' S_d of equation (2), which is a property of the electron gas, the 'phonon-drag thermopower' S_g is based on the interaction between electrons and phonons. (A current of phonons will drag electrons along, and thereby cause a contribution to the Seebeck coefficient.) This contribution is generally observed below room temperature, and its sign may or may not coincide with the sign of the diffusion thermopower.

4. Summary

We have prepared NbIrSn and NbIrSb, two new members of a family of compounds with a cubic MgAgAs-type structure. Their lattice parameters are 617.76(2) and 614.97(2) pm, respectively. Both compounds exhibit incongruent melting behaviour. NbIrSn is a p-type semiconductor with an energy gap of 0.28 eV. NbIrSb has metallic transport properties. The Seebeck coefficient of NbIrSb may be explained in terms of a free-electron model, with an additional phonon-drag contribution below room temperature. The formation of the solid solutions $NbIrSn_{1-x}Sb_x$ has been confirmed for $x = 0.01$ and 0.5.

References

[1] Villars P and Calvert L D 1991 *Pearson's Handbook of Crystallographic Data for Intermetallic Phases* 2nd edn, vols 1–4 (Metals Park, OH: ASM International)

[2] Dwight A E, Mueller M H, Conner R A Jr, Downey J W and Knott H 1968 *Trans. Metall. Soc. AIME* **242** 2075–80

[3] Jeitschko W 1970 *Metall. Trans.* **1** 3159–62

[4] Dwight A E 1974 *J. Less-Common Met.* **34** 279–84

[5] Marazza R, Ferro R and Rambaldi G 1975 *J. Less-Common Met.* **39** 341–5

[6] Stadnyk Yu V, Mykhailiv L A, Kuprina V V and Skolozdra R V 1989 *Inorg. Mater.* **24** 1196–8

[7] Skolozdra R V, Stadnyk Yu V, Gorelenko Yu K and Terletskaya E E 1990 *Sov. Phys.–Solid State* **32** 1536–8

[8] Kuentzler R, Clad R, Schmerber G and Dossmann Y 1992 *J. Magn. Magn. Mater.* **104–107** 1976–8

[9] Evers C B H, Richter C G, Hartjes K and Jeitschko W 1997 *J. Alloys Compounds* **252** 93–7

[10] Dudkin L D, Dashevskii Z M and Skolozdra R V 1993 *Inorg. Mater.* **29** 249–53

[11] Aliev F G, Brandt N B, Moshchalkov V V, Kozyrkov V V, Skolozdra R V and Belogorokhov A I 1989 *Z. Phys.* B **75** 167–71

[12] Toboła J, Pierre J, Kaprzyk S, Skolozdra R V and Kouacou M A 1998 *J. Phys.: Condens. Matter* **10** 1013–32

[13] Cook B A, Harringa J L, Tan Z S and Jesser W A 1996 *Proc. 15th Int. Conf. on Thermoelectrics, ICT96* (Piscataway, NJ: IEEE) pp 122–7

[14] Hohl H, Ramirez A P, Kaefer W, Fess K, Thurner Ch, Kloc Ch and Bucher E 1997 *MRS Symp. Proc.* vol 478, ed T Tritt *et al* (Pittsburgh, PA: Materials Research Society) pp 109–14
[15] Uher C, Hu S, Yang J, Meisner G P and Morelli D T 1997 *Proc. 16th Int. Conf. on Thermoelectrics, ICT97* (Piscataway, NJ: IEEE) pp 485–8
[16] Drys M 1978 *J. Less-Common Met.* **58** 173–7
[17] West A R 1989 *Solid State Chemistry and its Applications* (Chichester: Wiley)
[18] Blatt F J, Schroeder P A, Foiles C L and Greig D 1976 *Thermoelectric Power of Metals* (New York: Plenum)